Study on Optimal Condition of Adaptive Maximum Torque Per Amp Controlled Induction Motor Drives

Chun-Ki Kwon[†]

Abstract – Adaptive Maximum Torque Per Amp (Adaptive MTPA) control for induction motor drives seeks to achieve a desired torque with the minimum possible stator current regardless of operating points. This is favorable in terms of inverter operation and nearly optimal in terms of motor efficiency. However, the Adaptive MTPA control was validated only from the viewpoint of tracking a desired torque and was not shown that the desired torque is achieved with minimum possible stator current. This work experimentally demonstrates that optimal condition for Adaptive Maximum Torque Per Amp Control Strategy is achieved regardless of rotor resistance variation.

Keywords: Induction motor model, Optimal control, Adaptive maximum torque per amp (MTPA) control, Maximum torque per amp condition

1. Introduction

Highly efficient operation of induction motor has been studied in the past years [1-6]. Among many efforts to obtain optimal performance, an Adaptive Maximum Torque Per Amp (Adaptive MTPA) control of induction motor drives was proposed [7]. One interesting approach to develop an Adaptive MTPA control is to employ an alternate *qd* induction machine model (AQDM) rather than the classical *qd* model (CQDM), such as in [8-11]. The Adaptive MTPA control strategy set forth in [7] has demonstrated the ability to achieve the commanded torque with good accuracy, regardless of temperature variation.

However, efforts have been made to develop many control algorithms for tracking a desired torque, particularly in the case of optimal controls [1-6, 8]. Little study has been conducted on the optimality of the MTPA control that the desired torque was achieved with minimum possible stator current [1-6, 8].

Thus, this work demonstrates its optimality in a way that maximum torque was achieved for a certain stator current, which is also called maximum torque per amp condition. In addition, satisfaction of maximum torque per amp condition is also shown as rotor resistance is varied.

2. Alternate QD Induction Machine (AQDM)

Alternate QD Model (AQDM) included leakage saturation, magnetizing saturation, and distributed system effects in the rotor circuits which CQDM in [8-13] failed to represent over all possible operating conditions due to its constant parameters. Stator and rotor leakage inductance, and the absolute inverse magnetizing inductance are expressed as function of magnitude of magnetizing flux linkage, λ_m, which is equal to $\sqrt{2}\left|\tilde{\lambda}_{qm}\right|$. Stator and rotor leakage inductance, and the absolute inverse magnetizing inductance are denoted as $L_{ls}(\lambda_m)$, $L_{lr}(\lambda_m)$, and $\Gamma_m(\lambda_m)$, respectively. To consider distributed system effects in the rotor circuits, the rotor impedance, $Z_r(j\omega_s)$ in Laplace form. $Z_r(j\omega_s)$ is separated into a real and imaginary part, which are denoted $r_r(j\omega_s)$ and $j\omega_s L_{lrz}(j\omega_s)$, respectively.

The steady-state equivalent circuit representing the AQDM in [14] is shown in Fig. 1. Additional details on the AQDM model and its nomenclature are found in [14, 15]. In this work, the functional forms for AQDM parameters are specified as follows:

$$L_{ls} = l_{s1} \tag{1}$$

$$L_{lr}(\lambda_m) = l_{r1} + \frac{l_{r2}}{1 + (l_{r3}\lambda_m)^{l_{r4}}} \tag{2}$$

$$\Gamma_m(\lambda_m) = m_1 - m_2\lambda_m + e^{m_3(\lambda_m - m_4)} + e^{m_5(\lambda_m - m_6)} \tag{3}$$
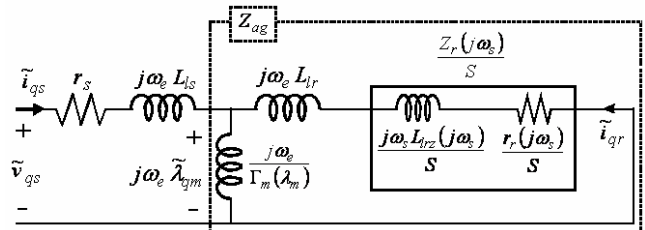

Fig. 1. Steady-state equivalent circuit of AQDM model with rotor impedance represented as $r_r(j\omega_s) + j\omega_s L_{lrz}(j\omega_s)$

†   Corresponding Author: Dept. of Medical Information Technology Engineering, Soonchunhyang University, Korea. (chunkikwon@ sch.ac.kr)

$$Y_r\left(s=j\omega_s\right)=\frac{1}{Z_r\left(s=j\omega_s\right)}$$

$$=\frac{y_{a1}}{y_{b1}s+1}+\frac{y_{a2}}{y_{b2}s+1}+\frac{y_{a3}}{y_{b3}s+1}\qquad(4)$$

The parameters in (1)-(4) of AQDM were characterized by applying fitting process to the functional forms of (1)-(4) on the laboratory experimental data taken for a 4-pole, 460 V, 50 Hp, 60 Hz, delta-connected squirrel cage induction motor. The resultant parameters in (1)-(4) of AQDM for the test induction motor are listed in Table 1 and are illustrated in Fig. 2. Detailed procedures of the parameter identification for AQDM is set forth in [14, 16] but is omitted due to limited space.
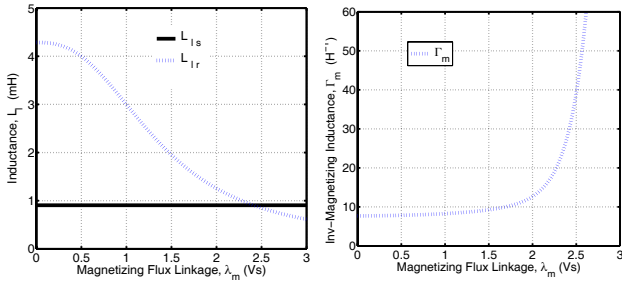
(a) Stator and Rotor leakage inductance

(b) Inverse Magnetizing inductance
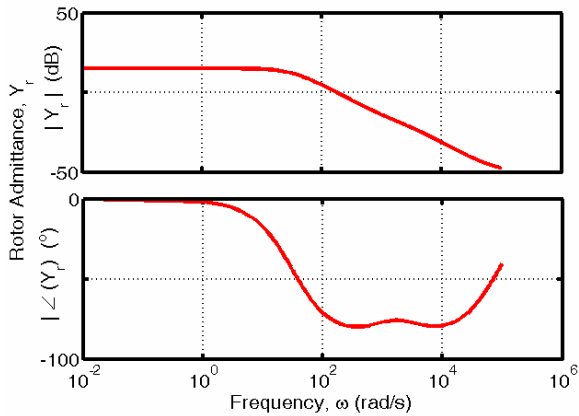
(c) Rotor admittance inductance

Fig. 2. AQDM parameters for the test induction motor

Table 1. Resultant parameters

$L_{ls}(\cdot)$		$\Gamma_m(\cdot)$		$Y_r(\cdot)$	
l_{s1}	9.06e-4	m_1	6.79e0	y_{a1}	5.65e0
$L_{lr}(\cdot)$		m_2	6.62e-1	y_{b1}	3.21e-2
l_{r1}	1.40e-4	m_3	5.03e0	y_{a2}	4.40e-2
l_{r2}	4.15e-3	m_4	1.85e0	y_{b2}	4.78e-4
l_{r3}	7.35e-1	m_5	8.68e-1	y_{a3}	3.17e-3
l_{r4}	2.59e0	m_6	1.29e-1	y_{b3}	8.76e-8

3. Adaptive Maximum Torque per Amp Control Strategy

3.1 Objective and structure

The structure of Adaptive MTPA control strategy is to express root-mean-square magnitude of the stator current I_s and slip frequency ω_s, as functions of the commanded torque and rotor resistance estimate $\hat{r}_r$ as shown in Fig. 3.

Its objective is to produce a desired torque with minimum stator current regardless of rotor resistance. To this end, two properties should be satisfied. One property is the tracking property and the other optimal condition in MTPA control strategy.

3.1.1 Tracking property

The tracking property is to achieve a desired torque at steady states for the current of I_s^*, the slip frequency of ω_s^*, and the estimated rotor resistance of $\hat{r}_r$ in the control strategy.

$$\left\|T_e\left(\omega_s^*,\ I_s^*,\ \hat{r}_r\right)\ -\ T_e^*\right\|\ <\ \varepsilon\qquad(5a)$$

Herein, ε is a very small number. As can be seen in Fig. 4, torques at point B and C does not achieve torque command T_e^*, resulting in failure of the tracking property. However, torques at points A and A' satisfies this property.
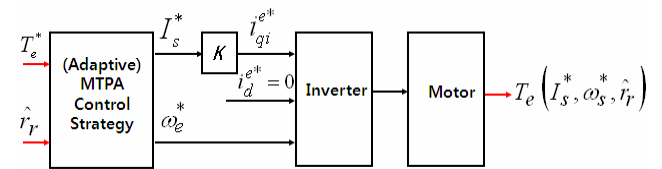

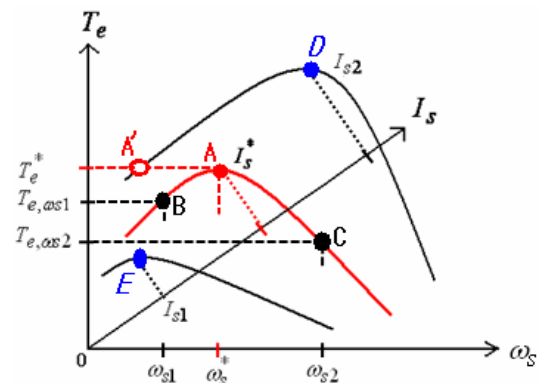**Fig. 3.** Structure of adaptive maximum torque per amp control strategy

Fig. 4. Optimal condition of (Adaptive) Maximum Torque Per Amp controlled induction machine drive

3.1.2 Optimal condition: MTPA condition

The other is optimal condition in MTPA control strategy at which condition the generated torque $T_e\left(I_s^*,\ \omega_s^*,\ \hat{r}_r\right)$ is not only the desired torque but also maximum torque for a given stator current of I_s^*. This is also called Maximum Torque Per Amp (MTPA) condition which the control strategy was named after. In other words, the desired torque was achieved with minimum stator current by minimizing conduction loss

$$T_e\left(I_s^*,\ \omega_s^*,\ \hat{r}_r\right)\ =\ \max_{I_s,\,\omega_s}\left\{T_e\left(I_s,\omega_s,\hat{r}_r\right)\right\} \qquad (5b)$$

In Fig. 4, the desired torque was achieved at point A' with I_{s2} and at point A with I_s^*. Since I_{s2} is larger than I_s^*, operation with I_s^* has higher efficiency than the one with I_{s2} due to higher conduction loss. Thus, MTPA condition is satisfied ONLY at A point.

3.2 Derivation of torque equation

To derive Adaptive MTPA control strategy, we can start by expressing the general electromagnetic torque Eq. (6) in the synchronous reference frame in terms of rms magnitude of the applied stator current I_s, slip frequency ω_s, and rotor resistance estimate $\hat{r}_r$ as the generated torque in Fig. 3.

$$T_e=\frac{3}{2}\frac{P}{2}\left(\lambda_{dm}^e i_{qs}^e-\lambda_{qm}^e i_{ds}^e\right) \qquad (6)$$

The relationship between the *q*- axis stator current in the phasor representation, and the *q*- and *d*- axis currents in the synchronous reference frame [17] is

$$\sqrt{2}\,\tilde{i}_{qs}=i_{qs}^e-j\,i_{ds}^e \qquad (7)$$

By letting all the stator current in the q-axis through appropriate selection of the phase reference, (7) reduces to

$$\sqrt{2}\,I_s=i_{qs}^e \qquad (8)$$

where I_s is the magnitude of $\tilde{i}_{qs}$. Like relations of currents in (7), the magnetizing flux linkage may be expressed as

$$\sqrt{2}\,\tilde{\lambda}_{qm}=\lambda_{qm}^e-j\,\lambda_{dm}^e \qquad (9)$$

After the algebraic manipulation of (6)-(9), the electromagnetic torque may be rewritten in terms of stator current and magnetizing flux linkage phasor as

$$T_e=\frac{3}{2}P\ \text{Imag}\left(\overline{\tilde{\lambda}_{qm}}\,I_s\right) \qquad (10)$$

where the overbar ' $-$ ' indicates complex conjugate.

From the AQDM steady-state equivalent circuit in Fig. 1, $\tilde{\lambda}_{qm}$ is expressed as

$$\tilde{\lambda}_{qm}\left(\omega_s,I_s,r_r\right)=\frac{Z_{ag}\left(\lambda_m,\omega_s,r_r\right)}{j\,\omega_e}I_s \qquad (11)$$

where Z_{ag} is the impedance in parallel with two branches, $j\omega_e/\Gamma_m\left(\lambda_m\right)$ and $j\omega_e L_{lr}\left(\lambda_m\right)+Z_r\left(j\omega_s\right)/S$, resulting in

$$Z_{ag}\left(\lambda_m,\omega_s,r_r\right)=\cfrac{\omega_e}{-j\Gamma_m\left(\lambda_m\right)+\cfrac{\omega_s}{j\omega_s\,L_{lr}\left(\lambda_m\right)+\left(r_r+j\omega_s L_{lrz}\right)}} \qquad (12)$$

Thus, substitution of (11) into (10) yields the electromagnetic torque in terms of ω_s, I_s, and r_r.

$$T_e\left(\omega_s,I_s,r_r\right)=\frac{3}{2}P\ \text{Imag}\left(\overline{\left(\frac{Z_{ag}\left(\lambda_m,\omega_s,r_r\right)}{j\,\omega_e}I_s\right)}I_s\right) \qquad (13)$$

where, since $\lambda_m=\sqrt{2}\left|\tilde{\lambda}_{qm}\right|$, $\lambda_m\left(\omega_s,\,I_s,\,r_r\right)$ can be computed as

$$\left|\omega_e\,\lambda_m\right|=\sqrt{2}\left|I_s\cdot Z_{ag}\left(\lambda_m,\omega_s,r_r\right)\right| \qquad (14)$$

With these two non-linear simultaneous Eqs. (13) and (14), torque can be found when ω_s, I_s, and r_r are given. In this work, Newton-Raphson method was utilized to calculate $\lambda_m\left(\omega_s,I_s,r_r\right)$ in (14). But any useful nonlinear algebraic equation solver can be used.

3.3 Derivation of AQDM based MTPA Control

3.3.1 Setting up optimization problem

Thus, maximum torque can be obtained by finding optimal slip frequency, ω_s^* for the given stator current, I_s^*, and rotor resistance estimate, $\hat{r}_r$, by applying any optimization technique to (15)

$$\begin{array}{c}\textit{maximize}\\ \omega_s\in\left\{1,\cdots,4\right\}\end{array}\ \frac{3}{2}P\ \text{Imag}\left(\overline{\left(\frac{Z_{ag}\left(\lambda_m,\,\omega_s,r_r\right)}{j\,\omega_e}I_s\right)}I_s\right) \qquad (15)$$

Therein, ω_s can be any value in real numbers but confined from 0 *rad/s* to 4 *rad/s* by our experience in order to avoid finding a local maximizer. Note that maximization of the torque in (13) for a given stator current means the minimization of the current for a given torque. The processing to solve the optimal slip frequency, ω_s^*, will be repeated for all combinations of I_s and r_r. It is assumed
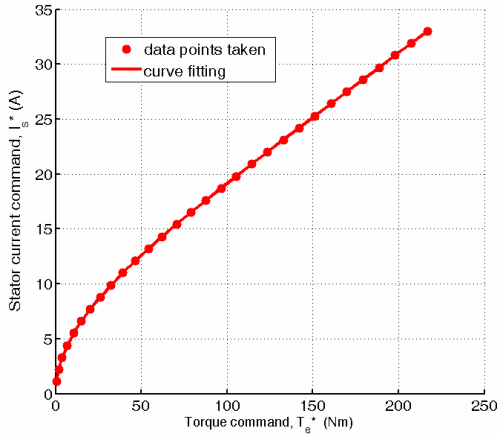
(a) Stator current command versus torque command
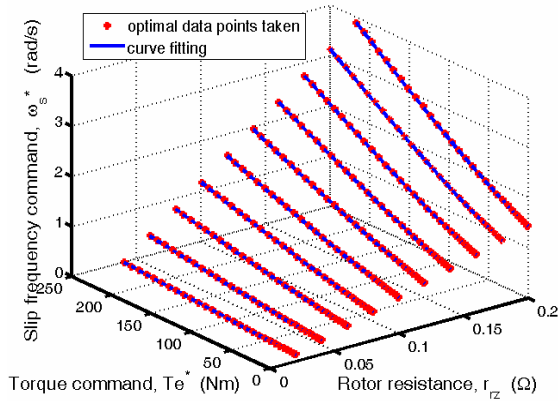
(b) Slip frequency command. vs. torque command and rotor resistance

Fig. 5. The control law and data points for Adaptive MTPA control strategy based on AQDM with different r_r

that I_s ranges from nearly 0 A to a somewhat over rated current and r_r is selected to vary from 0.01 Ω to 0.21Ω. The $j-$th point of I_s and $k-$th point of r_r will be denoted $I_{s,j}^*$ and $r_{r,k}$, respectively.

The optimal slip frequency, $\omega_{s,j,k}^*$, for a given pair of $\left(I_{s,j}^*, r_{r,k} \right)$ can be obtained by solving (15) with I_s and r_r replaced by $I_{s,j}^*$ and $r_{r,k}$. The resulting optimum slip frequency and the corresponding maximum value of torque for $I_{s,j}^*$ and $r_{r,k}$ will be denoted $\omega_{s,j,k}^*$ and $T_{e,j,k}^*$. These resulting data points are recorded for future data processing and are illustrated in Fig. 5.

3.3.2 Curve fitting

The data points { $I_{s,j}^*, T_{e,j,k}^*, r_{r,k}$ } in Fig. 5 (a) are used to construct a stator current control law. Note that I_s is not a function of r_r and so the form of stator current control law can be formulated as

$$I_s^* \left(T_e^* \right) = a_1 T_e^* + a_2 T_e^{*\,b_1} + a_3 T_e^{*\,b_2} \qquad (16)$$

where a_1, a_2, a_3, b_1, and b_2 are selected by maximizing the objective fitness function f_{AMTPA} defined as

$$f_{AMTPA} = \left(\varepsilon + \sqrt{\frac{1}{N_J} \sum_{j=1}^{N_J} \left| I_{s,j} - I_{s,j}^* \right|} \right)^{-1} \qquad (17)$$

where ε is a small number $\left(10^{-3} \right)$ added to the denominator in order to prevent singularities in the unlikely event of a perfect fit, N_J is the number of a set of the stator current command selected, and $I_{s,j}^*$ is given by (16) with $T_e^* = T_{e,j}^*$.

As for the slip frequency ω_s, it is a function of rotor resistance as well as the electromagnetic torque as shown in Fig. 5 (b). The data points { $\omega_{s,j,k}^*, T_{e,j,k}^*, r_{r,k}$ } are fit to the functional form

$$\omega_{s,AMTPA}^* \left(T_e^*, r_r^* \right) = d_0\, r_r^{*\,n1} + d_1\, r_r^{*\,n2}\, T_e^{*\,n3} \qquad (18)$$

where d_0, d_1, n_1, n_2, and n_3 are parameters to be identified. These parameters are identified by maximizing the objective function defined by (19)

$$f_{AMTPA} = \left(\varepsilon + \sqrt{\frac{1}{N_J\,N_K} \sum_{j=1}^{N_J} \sum_{k=1}^{N_K} \left| \omega_{s,j,k} - \omega_{s,j,k}^* \right|} \right)^{-1} \qquad (19)$$

where N_K is the number for a set of rotor resistances selected, and $\omega_{s,j,k}^*$ is given by (18) with $T_e^* = T_{e,j,k}^*$ and $r_r^* = r_{r,k}$. Both (16) and (18) are composed of the AQDM based Adaptive MTPA control law. To obtain coefficients in (16) and (18), any fitting technique could be used. In this work, a genetic algorithm is employed, which was part of the Genetic Optimization System Engineering Tool (GOSET 1.02), a Matlab based toolbox. Details are set forth in [18].

The resulting control laws for I_s^* and ω_s^* for the test machine may be expressed as

$$I_s^* \left(T_e^* \right) = 0.102\, T_e^* - 6.410\, T_e^{*\,0.011} + 7.790\, T_e^{*\,0.152} \qquad (20)$$

$$\omega_{s,AMTPA}^* \left(T_e^*, r_r^* \right) = 7.22 \cdot r_r^{*\,1.00} + 0.025\, r_r^{*\,1.00} \cdot T_e^{*\,1.15} \qquad (21)$$

and are also depicted, along with the individual data points, in Fig. 5. It can be seen that (20) and (21) fit the calculated data points { $I_{s,j}^*, \omega_{s,j}^*, T_{e,j}^*$ } in a good accuracy.

4. Test Set-up and Configuration for Study on Optimal Condition of Adaptive MTPA Control Strategy

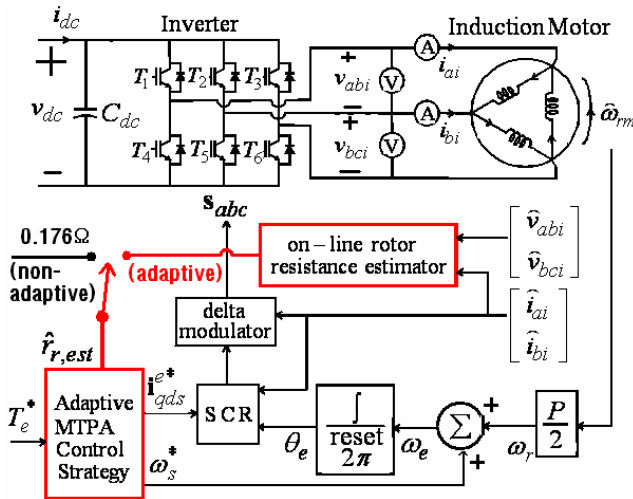The optimal condition of the proposed Adaptive MTPA control strategy was experimentally investigated. To this

Fig. 6. The configuration of the Non-Adaptive and Adaptive MTPA control based induction machine drive

end, a current controlled inverter-fed drive was used to operate the test induction motor. The configuration of the motor drive used in this study is depicted in Fig. 6. Therein, the upper part in Fig. 6 is the power converter topology. The lower part is composed of a speed control block with an anti-windup integrator, synchronous current regulator (SCR), and delta modulator, to determine the switching signal for switching devices, $T_1 \sim T_6$.

For this study, the optimal condition of the Adaptive MTPA control strategy was compared with that of the MTPA control strategy whose slip frequency, ω_s^*, control be obtained by substituting the value of 0.176 Ω for rotor resistance, r_r, in (21), as in Fig. 4. Thus, it results in

$$\omega_{s,MTPA}^* \left(T_e^* \right) = 1.2707 + 0.0044 \cdot T_e^{*\,1.15} \qquad (22)$$

in [7]. Herein, 0.176 Ω is the value of the rotor resistance at the temperature of 43 ℃ at which the test induction motor was characterized. For convenience purposes, MTPA control strategy is referred to as Non-Adaptive in that the commanded current and slip frequency are not adaptive to rotor resistance variation.

Additional details on the configuration for the drive and nomenclature are set forth in [16]. Fig. 7 shows the experimental set-up for this work. The induction motor being tested is enclosed in the small chamber and is exactly same as the motor used for the dynamometer.

The experiment focuses on a single operating condition. As shown in Fig. 8, the test induction machine was driven at a speed of 900 rpm and the torque command was set to 150 Nm in both cases. The torque estimator used in this work was shown to be highly accurate when the induction motor is rotating at moderate to high speeds [19-20].

With the experimental setup mentioned above, due to the difficulty in directly measuring the actual rotor resistance of the test motor, the rotor resistance estimator proposed in
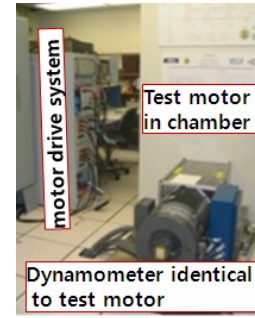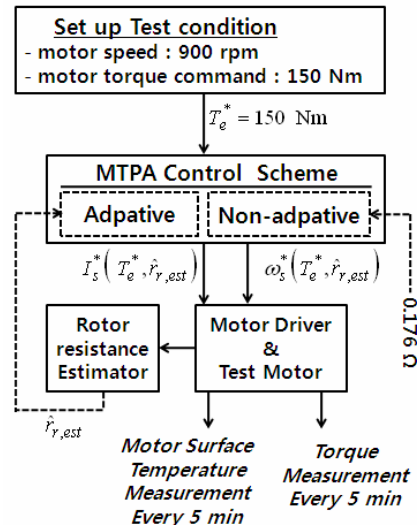

Fig. 7. Experimental set-up snapshot

Fig. 8. Experimental flow chart

[21] was utilized and incorporated into the proposed control strategy.

5. Review of Tracking Performance of Adaptive MTPA Control Strategy

To help readers understand the performance of the Adaptive MTPA control strategy, the results demonstrated in [7] are rewritten in this section. In [7], the Adaptive MTPA control strategy was validated by comparing its performance to that of the MTPA control strategy with slip frequency control law of (22).

As in Fig. 9, the performance for the two controls was recorded as the stator surface temperature varies. Therein, the red solid line with dot marks indicates the resultant torque of the Adaptive MTPA control strategy whose slip frequency command is $\omega_{s,AMTPA}^*$ in (21) and the dashed line indicates the resultant torque of the Non-Adaptive MTPA control strategy whose slip frequency command is $\omega_{s,MTPA}^*$ in (22). As can be seen, Adaptive MTPA control strategy produced the resultant torque closer to the torque command of 150 Nm and larger than resultant torque which the Non-Adaptive MTPA control strategy
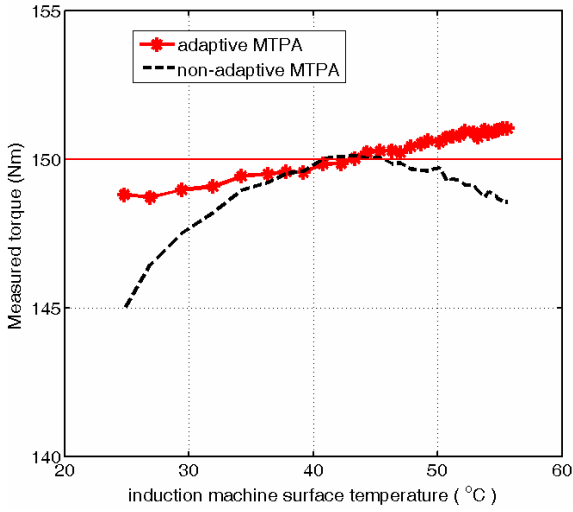
Fig. 9. Performances by the Adaptive MTPA control strategy and Non-Adaptive MTPA control strategy at the torque command of 150 Nm

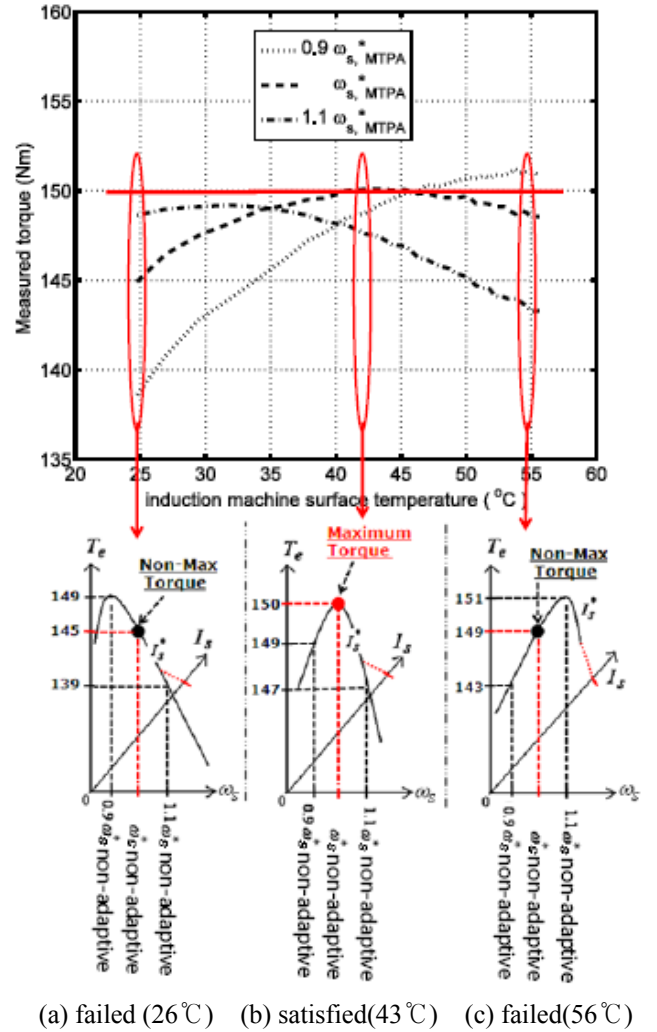## 6. Study on Optimal Condition of MTPA Control Strategy due to Rotor Temperature Variation

It would be of interest to investigate how MTPA condition is affected by rotor temperature variation.

6.1 MTPA condition of Non-Adaptive MTPA control strategy

Fig. 10 shows that the resultant electromagnetic torques at estimated optimal slip frequency command, $\omega_{s,MTPA}^*$, in (22) as well as two additional sets of resultant torques taken at 0.9 and 1.1 times of $\omega_{s,MTPA}^*$. In the initial part of each study as in Fig. 10 (a), when the temperature is low and where rotor resistance is smaller than the rotor resistance used to design Non-adaptive MTPA control strategy, the largest torque and closest to the commanded torque was not produced at $\omega_{s,MTPA}^*$ but at 0.9 times $\omega_{s,MTPA}^*$, resulting in failure of MTPA condition. Likewise, at the last part of the studies, the largest torque was again obtained at 1.1 times $\omega_{s,MTPA}^*$, which also means failure of MTPA condition. However, for some temperature region, maximum torque per ampere condition is in fact achieved at the estimate optimal slip frequency command $\omega_{s,MTPA}^*$. In the middle part of the study as in Fig. 10 (b), when rotor resistance was close to the design value, it can be seen that a slip value of $\omega_s = \omega_{s,MTPA}^*$ yields the most torque, thus satisfying MTPA condition.

6.2 MTPA condition of adaptive MTPA control strategy

The study on optimal condition, which is Maximum Torque Per Amp condition, of the proposed Adaptive MTPA control strategy was made by comparing its MTPA

(a) failed (26℃) (b) satisfied(43℃) (c) failed(56℃)

Fig. 10. MTPA conditions along temperature variation with T_e^* =150 (Nm) when controlled by Non-Adaptive MTPA control

condition to that of the Non-Adaptive MTPA control strategy to show optimal control of the Adaptive MTPA control strategy. Fig. 11 illustrates the MTPA condition of the two controls as the stator surface temperature increased during the duration of the study. The red solid line with dot marks indicates the estimated torque of the Adaptive MTPA control strategy whose slip frequency command is $\omega_{s,AMTPA}^*$ given by (21). For Non-Adaptive MTPA control strategy, three sets of estimates over neighborhoods of $\omega_{s,MTPA}^*$ in (22) have been included to investigate the satisfaction of the Maximum Torque Amp Condition. Therein, the dashed line indicates the estimated torque of the non-adaptive MTPA control strategy whose slip frequency command is $\omega_{s,MTPA}^*$ given by (22). In the initial part of study, when the temperature is low and where rotor resistance is smaller than the rotor resistance used to design Non-Adaptive MTPA control strategy, the torque estimated at 0.9 times of $\omega_{s,MTPA}^*$ is largest (of the non-adaptive controls). In the middle part (in time) of the study, when
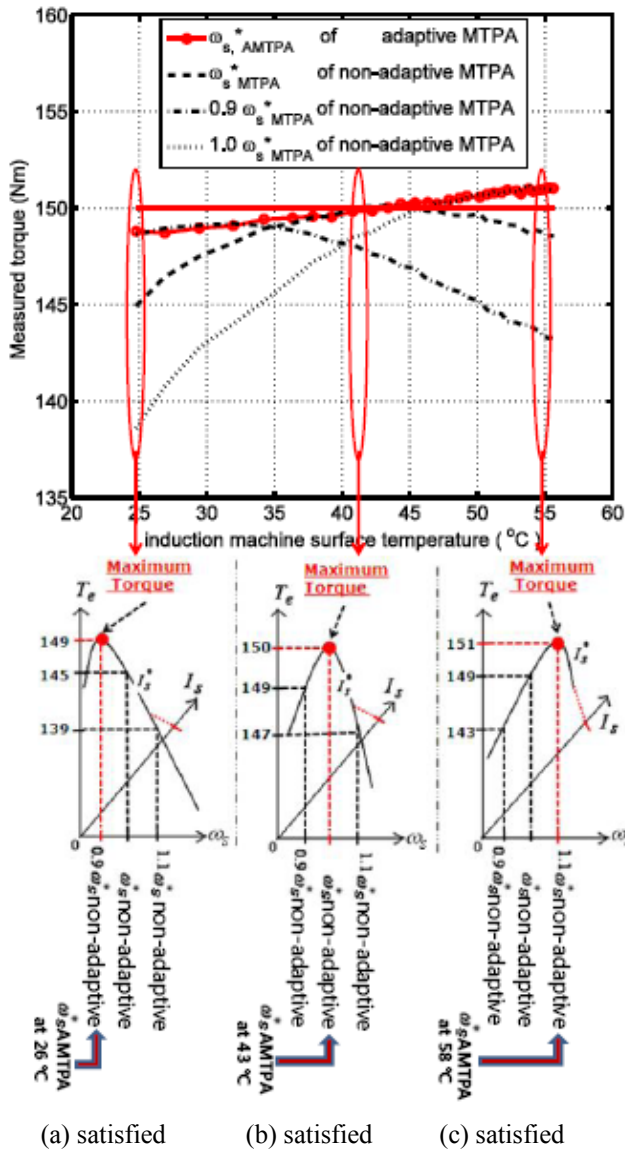
Fig. 11. MTPA conditions along temperature variation when controlled by Adaptive MTPA control strategy with T_e^* =150Nm

the rotor resistance was close to the design value, it can be seen that a slip value of $\omega_s = \omega_{s,MTPA}^*$ in (22) yields the most torque (again, at the Non-Adaptive controls). Finally, as the studies proceed in time, eventually the largest torque estimate was obtained using 1.1 times of $\omega_{s,MTPA}^*$. On the other hand, Adaptive MTPA control strategy adjusted the slip frequency command, $\omega_{s,AMTPA}^*$, given by (21) such that the largest torque are always achieved at $\omega_{s,AMTPA}^*$, thus satisfying MTPA condition.

The observations from Fig. 11 indicate that the Adaptive MTPA control strategy satisfies MTPA condition regardless of rotor temperature variation as well as achieve the desired torque accurately as validated in [7].

7. Conclusion

It was experimentally shown that the Adaptive MTPA control strategy performs optimally regardless of rotor resistance variation by showing that the torque produced at the optimal slip frequency is the largest and desirable at the same time, indicating that optimal condition (MTPA condition) of Adaptive MTPA control strategy is satisfied.

As can be seen from experimental results in the previous section, the Adaptive MTPA control strategy makes true optimal performance regardless of rotor resistance variation by reflecting rotor resistance variation in the design of optimal slip frequency control law.

Acknowledgements

References

[1] M. N. Uddin, Sang Woo Nam, "New Online Loss-Minimization-Based Control of an Induction Motor Drive," *IEEE transactions on Power Electronics*, Vol. 23, March 2008, pp. 926-933.

[2] C. Gonzalez, J. Arribas, and D. Prieto, "Optimal Regulation of Electric Drives With Constant Load Torque," *IEEE transactions on Industrial Electronics*, Vol. 53, No. 6, December 2006, pp. 1762-1769.

[3] G. Mino-Aguilar, J.M. Moreno-Eguilaz, B. Pryymak, and J. Peracaula, "An induction motor drive in-cluding a self-tuning loss-model based efficiency controller," *Applied Power Electronics Conference and Exposition, APEC 2008,* Feb 2008, pp. 1119-1125

[4] O. S. Ebrahim, M. A. Badr, A. S. Elgendy, P. K. Jain, "ANN-Based Optimal Energy Control of Induction Motor Drive in Pumping," *IEEE transactions on Energy Conversion*, Vol. 25, No. 3, 2010, pp. 652-660.

[5] J. Miao, H. Li, S. Chen, "Study on Efficiency Opti-mization Control of Induction Motor Drive System," *Control and Decision Conference, July* 2008, pp. 3244-3247

[6] B. Mirafzal, G. L. Skibinski, R.M. Tallam, "Deter-mination of Parameters in the Universal Induction Motor Model," *Indusstry Applications Conference, 2007, 42ⁿᵈ IAS Annual Meeting, Conference Record of the 2007 IEEE*, September 2007, pp.1207- 1216

[7] C. Kwon, "Study on an Adaptive Maximum Torque Per Amp Control Strategy for Induction Motor

Drives".

[8] *Journal of Electrical Engineering Technology,* Vol. 8, No. 1, January, 2013, pp. 110-117.

[9] O. Wasynczuk, S.D. Sudhoff, K.A. Corzine, J.L. Tichenor, P.C. Krause, I.G. Hansen, and L.M. Taylor, "A Maximum Torque Per Ampere Control Strategy for Induction Motor Drives," *IEEE Transactions on Energy Conversion*, Vol. 13, No. 2, June 1998, pp. 163-169.

[10] M. O. Sonnaillon, G. Bisheimer, C. De Angelo, G. O. Garcia, "Online Sensorless Induction Motor Temperature," *IEEE transactions on Energy Conversion*, Vol. 25, No. 2, 2010, pp. 273-280.

[11] Z. Gao, T. G. Habtler, and R. G. Harley, "A Complex Space Vector Approach to Rotor Temperature Estimation for Line-Connected Induction Machines With Impaired Cooling," *IEEE Transaction on industrial electronics*, Vol. 56, Jan. 2009, pp. 239-247.

[12] B. Karanayil, M. F. Rahman, and C. Grantham, "Online Stator and Rotor Resistance Estimation Scheme Using Artificial Neural Networks for Vector Controlled Speed Sensorless Induction Motor Drive," *IEEE transactions on Industrial Electronics*, Vol. 54, No. 1, February 2007, pp. 167-176.

[13] T. A. Najafabadi, F. R. Salmasi, P. Jabehdar-Maralani, "Detection and Isolation of Speed-, DC-Link Voltage-, and Current-Sensor Faults Based on an Adaptive Observer in Induction-Motor," *IEEE Transaction on industrial electronics*, Vol. 58, No. 5, 2011, pp. 1662-1672.

[14] T. Orlowska-Kowalska, M. Dybkowski, "Stator-Current-Based MRAS Estimator for a Wide Range Speed-Sensorless Induction-Motor," *IEEE Transaction on industrial electronics*, Vol. 57, No. 4, 2010, pp. 1296-1308.

[15] S. D. Sudhoff, P. L. Chapman, D. C. Aliprantis, and B. T. Kuhn, "Experimental Characterization Procedure for Use with of an Advanced Induction Machine Model," *IEEE Transactions on Energy Conversion*, Vol. 18, Mar 2003, pp. 48-56.

[16] S. D. Sudhoff, D. C. Aliprantis, B. T. Kuhn and P. L. Chapman, "An Induction Machine Model for Predicting Inverter-Machine Interaction," *IEEE Transactions on Energy Conversion*, Vol. 17, June 2002, pp. 203-210

[17] C. Kwon, S. D. Sudhoff, "Genetic Algorithm-Based Induction Machine Characterization Procedure With Application to Maximum Torque Per Amp Control," *IEEE Transactions on Energy Conversion*, Vol. 21, June 2006, pp. 405-415

[18] P. C. Krause, O. Wasynczuk, S. D. Sudhoff, Analysis of Electric Machinery and Drive Systems, IEEE Press, 2002.

[19] "Energy Systems Analysis Consortium (ESAC) Genetic Optimization System Engineering Tool (GOSET) Ver 1.02," School of Electrical and Computer Engr., Purdue Univ., West Lafayette, IN, 47907, 2003.

[20] J. Kim, J. Choi, and S. Sul, "Novel Rotor Flux Observer Using Observer Characteristic Function in Complex Vector Space for Field Oriented Induction Motor Drives," *IEEE transactions on Industry Applications*, Vol. 38, September/October 2002, pp. 1334-1443.

[21] P. L. Jansen and R. D. Lorenz, "A Physically Insightful Approach to the Design and Accuracy Assessment of Flux Observer for Field Oriented Induction Machine Drives," *IEEE Transactions on Industry Applications*, Vol. 30, No. 1, January/February 1994, pp. 101-110.

[22] C. Kwon, S. D. Sudhoff, "An On-line Rotor Resistance Estimator for Induction Machine Drives," *the 2005 International Electric Machines and Drives Conference*, May 2005, pp. 391-397.

Chun-Ki Kwon received B.S. and M.S. degrees in electrical engineering from Korea University in 1992 and 1994, respectively. He is with Soonchunhyang University, Asan, Chungnam, Korea. His research interests include control and modeling of electric machines, and expands this area to medical engineering such as rehabilitation devices.